J. Fluid Mech. (1980), *vol.* 97, *part* 1, *pp.* 129–144
Printed in Great Britain

Laminar boundary-layer reattachment in supersonic flow. Part 2. Numerical solution

By P. G. DANIELS

Department of Mathematics, The City University,
St John Street, London EC1V 4PB

(Received 29 January 1979)

A possible model of the flow in the neighbourhood of a point of reattachment of a supersonic laminar boundary layer consists of a three-tiered 'triple-deck' structure in which the basic problem reduces to that of solving the incompressible boundary-layer equations in the lower deck, a region of lateral and streamwise extent $O(R^{-\frac{5}{8}})$ and $O(R^{-\frac{3}{8}})$, where R is a representative Reynolds number of the flow (Daniels 1979). The present paper describes a scheme for the numerical solution of this problem which provides evidence in support of the proposed model and quantitative values for the $O(R^{-\frac{1}{4}})$ correction to the base pressure in the flow upstream and the $O(R^{-\frac{3}{8}})$ correction to the position of reattachment relative to the point of intersection of the incoming shear layer and the wall. An important feature of the scheme is that it copes successfully with a flow which contains substantial reverse velocities.

1. Introduction

A recent study (Daniels 1979; hereinafter referred to as I) has suggested that a triple-deck structure of the type originally envisaged by Stewartson & Williams (1969) for the flow near a point of separation of a laminar boundary layer in supersonic flow may also provide a consistent model of the flow near a point of reattachment. The possible significance of the triple deck in this context had been recognized in the study of reattachment behind a backward-facing step by Messiter, Hough & Feo (1973), and in I it is shown that asymptotic solutions of the relevant equations can be formulated which are indeed consistent with the reattachment of the flow within the lower deck of the triple deck. The triple deck has lateral and streamwise length scales $O(\epsilon^3 l)$, where $\epsilon \ll 1$ is defined by

$$\epsilon^{-8} = R = U_\infty l/\nu_\infty, \tag{1.1}$$

and R is the Reynolds number of the flow based on a convenient length scale l and the velocity and kinematic viscosity of the external stream, denoted by U_∞ and ν_∞ respectively. The triple deck divides laterally into three decks, the upper deck of height $O(\epsilon^3 l)$ which is inviscid and irrotational, the main deck of the same height $O(\epsilon^4 l)$ as the boundary layer and the lower deck of height $O(\epsilon^5 l)$. The fundamental problem reduces to the solution of the incompressible boundary-layer equations in the lower deck and in I a model of reattachment is proposed in which these equations must be solved in a domain $0 < x < \infty$, $0 \leqslant y < \infty$, subject to a certain set of conditions at the boundaries of the region. Here x and y are scaled streamwise and lateral co-ordinates

0022-1120/80/4381-8290 $02.00

in the lower deck, the incoming shear layer being supposed to strike the wall ($y = 0$) at the origin $x = 0$. Here an inviscid region of dimension $O(\epsilon^4 l)$ provides most of the flow reversal but does not quite complete reattachment, as suggested in the earlier study of Burggraf (1970) and that of Messiter *et al.* (1973). These studies were concerned with the overall features of specific flow models rather than the actual flow in the reattachment region. In I the possibility that a triple-deck structure governs the latter is considered and it is shown that asymptotic solutions of the triple-deck equations as $x \to 0+$ and $x \to \infty$ may be constructed which are consistent with reattachment at a finite value of x. The triple-deck problem, as posed in I, is quite independent of the solution in the surrounding regions of flow and it is therefore possible, and it is our intention here, to consider its solution in isolation from the remainder of any specific overall flow. It should be stressed, therefore, that there is no guarantee that the present model of reattachment will necessarily fit into any specific overall flow pattern; as with any singular perturbation problem involving matched asymptotic expansions, a consistent solution throughout the entire flow field is only guaranteed when the solution in each region matches with solutions in all the surrounding regions. No such complete pattern has yet been found for configurations such as backward-facing steps, compression ramps or shock-wave boundary-layer interactions, although Messiter *et al.* (1973) suggest that their inviscid model, which is consistent with the assumptions of, and indicated the presence of, the triple-deck structure considered here and in I, may apply to such situations. Certainly in the case of a compression ramp or shock-wave interaction, some features of the model, such as the backward jet which emanates from the inviscid zone, appear to contradict the assumptions concerning the flow upstream and it is by no means clear that a consistent overall flow can be obtained. A further discussion of some of the problems involved is given by Smith (1979). By showing that the triple deck does apparently provide one possible mechanism for reattachment, the results of I and of the present study do tend to support the model of reattachment proposed by Messiter *et al.* (1973) but clearly do not guarantee its overall consistency in any way.

Many numerical solutions of lower-deck problems have followed the method originally devised for the separation problem by Stewartson & Williams (1969), the injection solutions of Smith (1974) and trailing-edge solutions of the present author (1974) providing examples in the supersonic case. Here the outer boundary condition (at $y = \infty$) is dependent only upon the local value of x in contrast to the corresponding incompressible or subsonic flow (cf. Jobe & Burggraf 1974; Smith 1977). The major difficulties encountered with problems which involve separation and reattachment are concerned with the regions of reverse flow where the equations are no longer parabolic in the positive-x direction. Williams (1975) has improved his original separation solutions by extending his computational scheme into the reverse flow region beyond separation using the method developed by Flügge-Lotz & Reyhner (1968) in which the nonlinear momentum term $u\partial u/\partial x$ is neglected wherever $u < 0$. Provided that the reverse flow is small, this solution may then be used as an initial approximation in which the final solution is developed iteratively using a series of upstream and downstream sweeps of the flow region. However, in the reattachment problem envisaged here, the reverse flow velocity u in the lower deck is $O(x^{-1})$ as $x \to 0+$ (see § 2 below) and it is unlikely that a similar treatment will suffice. Instead a more general method of the type devised by Klemp & Acrivos (1972) for computing

boundary-layer flows containing reverse flow regions is required. There the domain is divided into regions of forward and reverse flow using an initial guess for the location $y = g(x)$ of the curve along which $u = 0$ and the solution computed in opposite directions from appropriate initial profiles in each region. A new estimate, based on the size of the discontinuity in the shear stress $\partial u/\partial y$, is then obtained for $g(x)$ and the whole procedure repeated until this discontinuity is reduced to a required tolerance.

The reattachment problem considered here is somewhat different from that of Klemp & Acrivos (1972) in a number of significant ways. First, the position of reattachment, x_R, is an unknown quantity which must be determined by the numerical scheme. Second, the outer boundary condition at $y = \infty$ is different from that of the boundary-layer problem of Klemp & Acrivos; this allows the value of $\partial u/\partial y$ along $y = g(x)$ to be made continuous throughout the iterative scheme and the outer boundary condition then automatically provides the new estimate for $g(x)$. Third, proper account must be taken of the severe singularity at $x = 0+$, where $p = O(x^{-2})$ and $u = O(x^{-1})$. Finally, as in a number of other triple-deck problems (see, for example, Smith 1974; Daniels 1974 and I) the lower deck pressure perturbation, p, must satisfy a prescribed boundary condition as $x \to \infty$, which in this case is $p \to 0$ as $x \to \infty$, and ensures that the triple-deck solution matches correctly with an attached boundary-layer flow downstream. The alternative would be the evolution of either the compressive solution in which separation occurs and p approaches a finite non-zero limit as $x \to \infty$, or the expansive solution which terminates in a singularity at a finite value of x (see Stewartson 1974).

A statement of the system and its asymptotic properties (derived in I) is made in § 2 and a full description of the numerical scheme in § 3. The results are presented in § 4 and are discussed in the light of experimental results in § 5.

2. Statement of the problem

We suppose a shear layer to be incident upon a wall $y^* = 0$ at the origin of a set of Cartesian axes x^*, y^*. Then it is argued in I that an inviscid zone of dimension $O(\epsilon^4 l)$ surrounding the origin evolves a three-tiered structure in the downstream direction $(x^*/\epsilon^4 \to \infty)$ which matches precisely with the three layers of a conventional triple deck where variations occur on the streamwise length scale

$$x = \left[\frac{(M_\infty^2 - 1)^{\frac{3}{8}}}{M_\infty^{\frac{3}{4}}} \left(\frac{\nu_w}{\epsilon^8}\right)^{\frac{1}{4}} \frac{\lambda_1^{\frac{3}{2}}}{\lambda^{\frac{1}{4}}}\right] \frac{x^*}{\epsilon^3}. \tag{2.1}$$

Here $\lambda_1 = M_0'(0)$, $\lambda = U_0'(0)$, where U_0 and M_0 are the velocity and Mach number profiles which evolve from the inviscid zone as $x^*/\epsilon^4 \to \infty$, with $U_0(\infty) = U_\infty$ and $M_0(\infty) = M_\infty$, the external velocity and Mach number of the supersonic flow outside the triple deck. ν_w is the kinematic viscosity of the fluid at the wall. A crucial assumption of the theory made in I is that $U_0(0) = 0$, the asymptotic form of the inviscid zone solution then suggesting that reattachment is not quite completed where $x^*/\epsilon^4 = O(1)$, thereby necessitating the presence of the triple deck downstream. In the triple deck, the fundamental problem reduces to the solution of the following system in the lower deck where x and

$$y = \left[\frac{(M_\infty^2 - 1)^{\frac{1}{8}}}{M_\infty^{\frac{1}{2}}} \left(\frac{\epsilon^8}{\nu_w}\right)^{\frac{1}{4}} \lambda^{\frac{1}{4}} \lambda_1^{\frac{1}{2}}\right] \frac{y^*}{\epsilon^5}, \tag{2.2}$$

are the order-one variables:

$$u\frac{\partial u}{\partial x}+v\frac{\partial u}{\partial y}=-\frac{dp}{dx}+\frac{\partial^2 u}{\partial y}, \quad \frac{\partial u}{\partial x}+\frac{\partial v}{\partial y}=0, \tag{2.3}$$

$$u=v=0 \quad \text{on} \quad y=0, \tag{2.4}$$

$$u\sim y-A(x) \quad \text{as} \quad y\to\infty, \tag{2.5}$$

$$p\sim -2/x^2 \quad \text{as} \quad x\to 0+, \tag{2.6}$$

$$p\to 0 \quad \text{as} \quad x\to\infty, \tag{2.7}$$

where $p(x)=A'(x)$. Here the physical velocity components u^*, v^* and pressure p^* are related to u, v and $p(x)$ by

$$\left.\begin{aligned} u^* &= \left[\frac{\epsilon M_\infty^{\frac{1}{2}}\lambda^{\frac{3}{4}}}{(M_\infty^2-1)^{\frac{1}{8}}\lambda_1^{\frac{1}{2}}}\left(\frac{\nu_w}{\epsilon^8}\right)^{\frac{1}{4}}\right]u(x,y), \\ v^* &= \left[\frac{\epsilon^3\lambda_1^{\frac{1}{2}}\lambda^{\frac{1}{4}}(M_\infty^2-1)^{\frac{1}{8}}}{M_\infty^{\frac{1}{2}}}\left(\frac{\nu_w}{\epsilon^8}\right)^{\frac{3}{4}}\right]v(x,y), \\ p^* &= p_\infty+\left[\frac{\epsilon^2\gamma p_\infty M_\infty\lambda_1}{(M_\infty^2-1)^{\frac{1}{4}}\lambda^{\frac{1}{2}}}\left(\frac{\nu_w}{\epsilon^8}\right)^{\frac{1}{2}}\right]p(x), \end{aligned}\right\} \tag{2.8}$$

where γ is the ratio of specific heats.

The boundary condition (2.4) is the no-slip condition at the wall while (2.5) represents the match with the solution in the main deck where $u=U_0+O(\epsilon)$, and incorporates the interaction with the supersonic flow outside the boundary layer which supplies the relation between the pressure and the displacement function $A(x)$. The condition (2.6) is required if the solution is to be consistent with that in the inviscid zone at $x=0$ while (2.7) ensures the evolution of an attached boundary-layer flow downstream of the triple-deck region.

The asymptotic properties of the lower-deck system have been derived in I and show that, as $x\to 0+$,

$$\begin{aligned} p &\sim -2x^{-2}+p_1+O(x^2|\log x|^{\frac{1}{2}}, x^2, \ldots), \\ A &\sim 2x^{-1}+p_1x+O(x^3|\log x|^{\frac{1}{2}}, x^3, \ldots), \end{aligned} \tag{2.9}$$

where p_1 is an arbitrary constant. The velocity field develops three distinct regions as $x\to 0+$, an inner viscous layer where $\eta=y/x=O(1)$ and

$$u\sim x^{-1}(4-6\tanh^2[\eta+C_0])+O(x, x|\log x|^{-\frac{1}{2}}, \ldots), \quad C_0=1{\cdot}146\ldots, \tag{2.10}$$

a transitional layer where $\theta=y/x|\log x|^{\frac{1}{2}}=O(1)$ and

$$u\sim -2x^{-1}+O(x|\log x|^{\frac{1}{2}}, x, \ldots), \tag{2.11}$$

and an outer layer where $y=O(x^{-1})$ and

$$\begin{aligned} \psi &\sim \{\tfrac{1}{2}y^2-2yx^{-1}\}-p_1xy+C_1+O(x^2|\log x|^{\frac{1}{2}}, x^2, \ldots), \quad C_1=1{\cdot}101\ldots, \\ u &\sim \{y-2x^{-1}\}-p_1x+O(x^3|\log x|^{\frac{1}{2}}, x^3, \ldots). \end{aligned} \tag{2.12}$$

Here ψ is the stream function defined by $u=\partial\psi/\partial y, v=-\partial\psi/\partial x$ and we see that the

boundary of the reverse flow region $y \sim 2/x$ is located half-way between the wall and the dividing streamline $\psi = 0$ where $y \sim 4/x$.

As $x \to \infty$,

$$p \sim -k(C_1 - 3p_1)x^{-\frac{4}{3}}, \quad A \sim 3k(C_1 - 3p_1)x^{-\frac{1}{3}}, \quad u = y + O(x^{-\frac{1}{3}}), \tag{2.13}$$

where $k = (-\frac{2}{3})!/3^{\frac{4}{3}}(-\frac{1}{3})! = 0{\cdot}317\ldots$, a flux argument having been used to relate the coefficients of p and A to the value of the unknown constant p_1 in the expansion of the pressure at $x = 0$. The value of p_1 is one of the results which can only be determined from the numerical solution of the system and provides an $O(\epsilon^2)$ correction to the pressure in the inviscid zone upstream. The two expansions (2.10) and (2.13) suggest that at some point $x = x_R$, with $0 < x_R < \infty$, the skin friction vanishes and reattachment occurs, although again a full numerical solution is the only way of establishing this behaviour conclusively and of determining the value of x_R, which is essentially the $O(\epsilon^3)$ correction to the distance of reattachment from the point of intersection of the incoming shear layer and the wall.

3. The numerical scheme

We suppose that the boundary of the reverse flow region (along which $u = 0$) is given by $y = g(x)$ and define

$$\bar{y} = y - g(x), \quad \bar{v} = v - ug'(x). \tag{3.1}$$

If reattachment occurs at $x = x_R$, we may suppose that $g = 0$ in the region $x > x_R$ so that there $\bar{y}$ and $\bar{v}$ may be identified with the original variables y and v. The system (2.3), (2.4), (2.5) becomes

$$\left.\begin{aligned} &u\frac{\partial u}{\partial x} + \bar{v}\frac{\partial u}{\partial \bar{y}} = -\frac{dp}{dx} + \frac{\partial^2 u}{\partial \bar{y}^2}, \quad \frac{\partial u}{\partial x} + \frac{\partial \bar{v}}{\partial \bar{y}} = 0, \\ &u = \bar{v} = 0 \quad \text{on} \quad \bar{y} = -g(x), \\ &u = 0 \quad \text{on} \quad \bar{y} = 0, \\ &u \sim \bar{y} + g - A \quad \text{as} \quad \bar{y} \to \infty, \end{aligned}\right\} \tag{3.2}$$

where $p = A'$, and we treat each of the three regions $\bar{y} < 0$, $x < x_R$ (I, reverse flow), $\bar{y} > 0$, $x < x_R$ (II, forward flow) and $\bar{y} > 0$, $x > x_R$ (III, forward flow) separately (see figure 1).

In region I the solution is computed by marching upstream in the negative x direction from x_R. Since the boundary of the region is a function of x, it is convenient to replace the variable $\bar{y}$ by a new variable ξ defined by

$$\xi = \bar{y}/g(x), \tag{3.3}$$

so that ξ varies between constant limits, $-1 \leqslant \xi \leqslant 0$. In view of the asymptotic properties of the solution at $x = 0+$ we also write

$$p = -2x^{-2} + p_1 + P(x), \quad g = 2x^{-1} + p_1 x + G(x). \tag{3.4}$$

The new variables P and G then remain finite throughout the region and may therefore

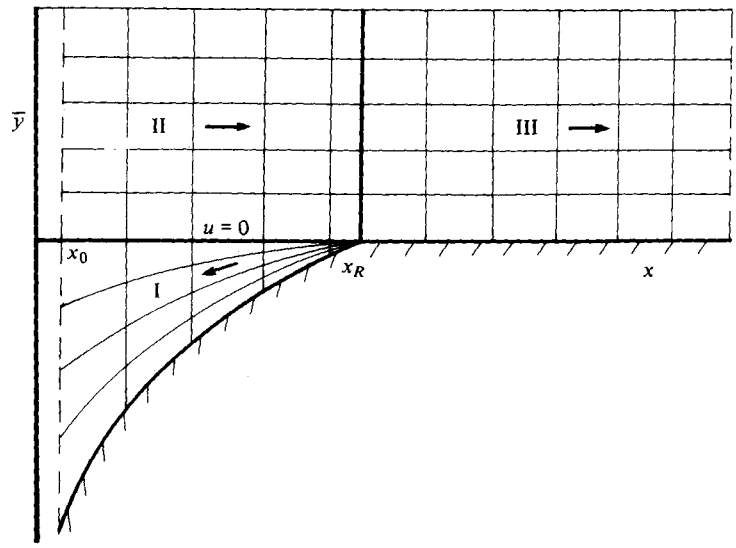

FIGURE 1. The mesh pattern and flow regions in the $x, \bar{y}$ plane.

be discretized accurately even near $x = 0$. Adopting a similar treatment for the streamwise velocity we write

$$u = x^{-1}U_1(x, \xi) \quad \text{for} \quad x \leqslant 1, \tag{3.5}$$

$$u = X^2 U_2(x, \xi) \quad \text{for} \quad 1 \leqslant x \leqslant x_R, \tag{3.6}$$

where $X = x - x_R$, and use the variables U_1 and U_2 for $x < 1$ and $x > 1$ respectively. The first caters for the asymptotic structure (2.12) as $x \to 0$ and the second for the neighbourhood of reattachment.

Near reattachment we expect

$$p \sim p(x_R) + aX, \quad g \sim -bX, \quad \text{as} \quad X \to 0-, \tag{3.7}$$

and, since $\partial u/\partial y(x, 0) \to 0$ as $X \to 0$,

$$\psi \sim cXy^2 + dy^3, \quad u \sim 2cyX + 3dy^2, \quad v \sim -cy^2, \quad \text{as} \quad X \to 0, \quad y \to 0. \tag{3.8}$$

Substitution into the equations of motion (2.3) and use of the fact that $u = 0$ on $y = g$ determines the two constants c and d in terms of a and b as

$$c = \tfrac{1}{4}ab, \quad d = \tfrac{1}{6}a. \tag{3.9}$$

Thus in terms of ξ we have

$$u \sim \tfrac{1}{2}ab^2X^2\xi(\xi + 1) \quad \text{for} \quad -1 \leqslant \xi \leqslant 0, \quad \text{as} \quad X \to 0-, \tag{3.10}$$

and the initial profile for U_2 in region I is

$$U_2(x_R, \xi) = \tfrac{1}{2}ab^2\xi(\xi + 1). \tag{3.11}$$

Incidentally it also follows from (3.9) and (3.8) that the zero streamline $\psi = 0$ lies along $y \sim -\frac{3}{2}bX$ as $X \to 0$ and thus the curve of zero streamwise velocity $y = g$ divides the region between the wall and the zero streamline in the ratio of 2:1 at the

point of reattachment. This ratio adjusts to 1:1 as the inviscid region is approached upstream [see (2.12)].

Provided the pressure gradient which drives the system and the boundary of the reverse flow region are specified (i.e. dP/dx and G are known functions of x) the solution for U_2 is computed upstream from the profile (3.11) by discretization of U_2, P and G in the system

$$\left.\begin{aligned} X^2\frac{\partial^2 U_2}{\partial\xi^2}-gX^2\frac{\partial U_2}{\partial\xi}\bar{v}_2-g^2\left(2X^3U_2^2+\tfrac{1}{2}X^4\frac{\partial}{\partial x}(U_2^2)+\frac{dP}{dx}+\frac{4}{x^3}\right)=0,\\ \bar{v}_2=\bar{v}-g'\xi X^2U_2=-X^2\left(\frac{dG}{dx}-\frac{2}{x^2}+p_1\right)\int_{-1}^{\xi}U_2\,d\xi-g\int_{-1}^{\xi}\left(X^2\frac{\partial U_2}{\partial x}+2XU_2\right)d\xi, \end{aligned}\right\} \tag{3.12}$$

onto a uniform mesh in x and ξ, using central differences in the x direction, the formula (3.4) for g and the trapezium rule for $\bar{v}$. At $x = 1$ the switch is made from U_2 to U_1, (3.12) now being replaced by

$$\left.\begin{aligned} x^2\frac{\partial^2 U_1}{\partial\xi^2}-gx^2\frac{\partial U_1}{\partial\xi}\bar{v}_1-g^2\left(\tfrac{1}{2}x\frac{\partial}{\partial x}(U_1^2)-U_1^2+x^3\frac{dP}{dx}+4\right)=0,\\ x^2\bar{v}_1=x^2\bar{v}-g'\xi xU_1=-x\left(\frac{dG}{dx}-\frac{2}{x^2}+p_1\right)\int_{-1}^{\xi}U_1\,d\xi-g\int_{-1}^{\xi}\left(x\frac{\partial U_1}{\partial x}-U_1\right)d\xi. \end{aligned}\right\} \tag{3.13}$$

At the current x step, the profile U_1 or U_2 is found from that at the previous upstream step, $x+\Delta x$, by use of Newton iteration to linearize the system, the matrix form of which is then reduced to one superdiagonal and solved by forward substitution.

From the solution in I we obtain the shear stress and normal velocity at $\bar{y} = 0-$,

$$\left.\begin{aligned} W(x)=\frac{\partial u}{\partial y}(x,g)&=(xg)^{-1}\frac{\partial U_1}{\partial\xi}(x,0)\quad\text{for}\quad x\leqslant 1\\ &=X^2g^{-1}\frac{\partial U_2}{\partial\xi}(x,0)\quad\text{for}\quad x\geqslant 1, \end{aligned}\right\} \tag{3.14}$$

$$V(x)=v(x,g)=\bar{v}(x,0), \tag{3.15}$$

the values of W being stored at the mesh points and those of V mid-way between mesh points. Provided that P and G conform to the asymptotic behaviour (2.9) we expect that $U_1 \sim 2\xi(-1 < \xi \leqslant 0)$, $W \sim 1$ and $V \sim -4/x^3$ as $x \to 0+$, the last of these being evident from (3.13). Clearly inaccuracies will develop as x decreases despite the transformations (3.4)–(3.6) and in practice the solution is terminated at $x = x_0$ ($x_0 > 0$). To continue the solution further, a more sophisticated treatment would be required to obtain adequate resolution of the inner viscous region at the wall, and this was not attempted.

In region II the solution now proceeds in the positive x direction from the initial profile

$$u=\bar{y},\quad 0\leqslant\bar{y}<\infty \tag{3.16}$$

at $x = x_0$, the asymptotic form (2.12) inferring that this is correct to algebraic order in x as $x \to 0+$ and thereby suggesting that relatively little inaccuracy is incurred in choosing even a relatively large value of $x_0 > 0$. An analogy with the method of Klemp & Acrivos (1972) would be to solve the system in II subject to $u = 0, \bar{v} = V$

on $\bar{y} = 0$ and the outer conditions (2.5) as $\bar{y} \to \infty$, using the same value of $g(x)$ as in I. The solution would supply values of $\partial u/\partial y(x, g)$ different from $W(x)$ and an iterative formula would be required to estimate a new $g(x)$ from this data; in the present problem a more straightforward procedure is to apply the shear stress values obtained from I directly so that the flow is automatically continuous along $\bar{y} = 0$. Thus we solve II using the boundary conditions

$$\left.\begin{aligned} &u = 0, \quad u_{\bar{y}} = W(x), \quad \bar{v} = V(x) \quad \text{on} \quad \bar{y} = 0 \\ &u_{\bar{y}} \to 1 \quad \text{as} \quad \bar{y} \to \infty \end{aligned}\right\} \quad \text{for} \quad x < x_R, \tag{3.17}$$

the additional condition at $\bar{y} = 0$ replacing the second outer boundary condition, which in terms of P and G becomes

$$u_x \to G' - P \quad \text{as} \quad \bar{y} \to \infty. \tag{3.18}$$

The system, which is discretized using central differences in the x direction, is

$$u\frac{\partial u}{\partial x} - \frac{\partial u}{\partial \bar{y}}\left\{\int_0^{\bar{y}} \frac{\partial u}{\partial x}\, d\bar{y} - V(x)\right\} + \frac{dP}{dx} + \frac{4}{x^3} - \frac{\partial^2 u}{\partial \bar{y}^2} = 0, \tag{3.19}$$

and is now solved for u, $\bar{v}$ and P using (3.17) and marching downstream in the positive x direction. The value of $u_x(x, \infty)$ then automatically determines a new estimate for the function $G(x)$ from (3.18). Note that the system (3.17), (3.19) is independent of the value of p_1 and is solved essentially subject to the conditions $P = 0$, $G = 0$ at $x = 0$. In practice the computation begins at x_0 but the asymptotic expansions of P and G involve x^2 and x^3 multiplied by infinite series of powers of $|\log x|^{\frac{1}{4}}$ [see (2.9) and I] and truncations of these series are unlikely to be accurate for x near x_0 unless x_0 is very small. However it seems reasonable to suppose that the major variation in P and G near x_0 will be of approximately second and third degree in x (respectively) and so starting values

$$P = a_0 x^2, \quad G = b_0 x^3 \tag{3.20}$$

were taken at $x = x_0$, the values of a_0 and b_0 being determined from the previous iteration. The computation now proceeds from x_0 using a uniform mesh in x and $\bar{y}$ to provide the velocity profile and pressure at $x = x_R$. Direct use of $W(x)$ ensures that the profile at x_R is one with zero skin friction at the wall and this is now used as the initial profile for the solution in region III which is computed downstream in a conventional manner using the dependent variables u and p, a uniform mesh in x and y and the full boundary conditions (2.4), (2.5). The attainment of the final boundary condition (2.7) as $x \to \infty$ depends upon the correct choice of the pressure at $x = x_R$, too high or low a value resulting in the evolution of a compressive or expansive solution (respectively). The correct choice is achieved by adjustment of p_1, for the actual pressure at x_R is

$$p(x_R) = P(x_R) - \frac{2}{x_R^2} + p_1, \tag{3.21}$$

and only $P(x_R)$ is fixed by the solution in II. In practice p_1 must be adjusted by trial and observation so that several computations in III are required for each single computation in I and II; note that since use of P and G renders the solution in II independent of p_1, no recomputation of this region is necessary during each complete iteration of the flow field.

The full scheme is now described as follows:

(1) make initial guesses for $G(x)$, $P(x)$, x_R and p_1 (G_0, P_0, x_{R0} and p_{10} respectively);

(2) solve in I using G, P, x_R and p_1 to obtain shear stress and normal velocity profiles $W(x)$ and $V(x)$ at $\bar{y} = 0$;

(3) solve in II using W and V to obtain new pressure $P(x) = P_n(x)$ and also new $G(x) = G_n(x)$ using (3.18);

(4) select a value of $p_1 = p_{1n}$ in (3.21) and solve for $u(x, y)$ and $p(x)$ in III;

(5) adjust p_{1n} and recompute in III until $p \to 0$ as $x \to \infty$ (to within a required tolerance);

(6) form the new values of P, G and p_1 from the old values and those obtained in stages 3–5 using a relaxation factor R, where

$$P = RP_0 + (1-R)P_n,$$

$$G = RG_0 + (1-R)G_n,$$

$$p_1 = Rp_{10} + (1-R)p_{1n};$$

(7) calculate the new value of x_R from the point at which the new

$$g(x) = G(x) + 2/x + p_1 x$$

vanishes;

(8) set $P_0 = P$, etc., return to stage 2 and repeat the whole procedure until successive iterates are identical to within a required tolerance.

The reattachment position x_R and the pressure coefficient p_1 are intended to converge to their true values and, provided the system is sufficiently under-relaxed and the initial guess for x_R is large enough, its value gradually decreases to the final limit with successive iterations. The discretization of regions I and II is arranged so that the mesh points are always at fixed locations except for those located along the line $x = x_R$, which vary as x_R varies. This means that the first x step in region I and the last x step in region II are generally shorter than the other steps, this being easily incorporated into the program.

4. Numerical results

The program was started from initial profiles $P = 0$ and

$$G = 0 \quad \text{for} \quad x \leqslant \tfrac{3}{2}, \quad G = -2x^{-1} + \tfrac{8}{9}(3-x) \quad \text{for} \quad \tfrac{3}{2} \leqslant x \leqslant 3, \tag{4.1}$$

with $x_{R0} = 3$, $p_{10} = 0$ and $a_0 = b_0 = 0$. The Newton iteration at each individual x step was computed to a tolerance of 10^{-7} in the values of the dependent variables. Step-sizes were initially set at $\Delta x = 0{\cdot}1$, $\Delta\xi = 0{\cdot}02$, $\Delta\bar{y} = 0{\cdot}1$ and $\Delta y = 0{\cdot}1$ and in regions II and III outer boundaries were taken at $\bar{y} = 7{\cdot}5$ and $y = 7{\cdot}5$. The small value of $\Delta\xi$ ensured adequate resolution of the inner boundary-layer structure (2.10) as the value of x decreased in I and for the same reason a relatively large value of $x_0 = 0{\cdot}4$ was chosen. In fact the approach of the shear stress W to its limiting value of 1 as $x \to 0$ was found to be rapid and was generally achieved to within the order of 10^{-4} at x_0 throughout the computation.

The major inaccuracies in the scheme are thought to stem from the severe truncation of the Taylor series expansions of the variables and the use of the trapezium

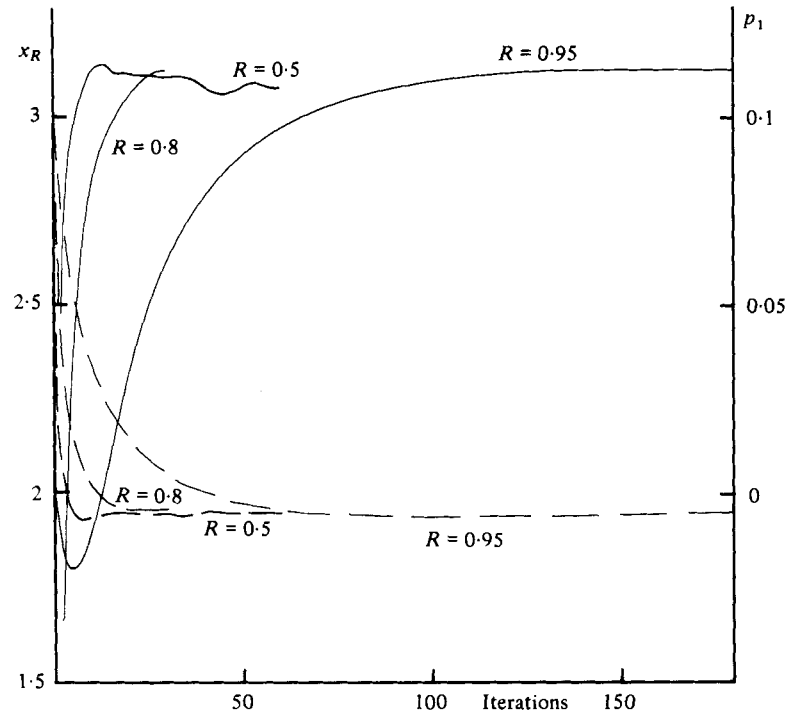

FIGURE 2. Convergence properties of x_R (– –) and p_1 (——) for various relaxation factors.

rule in the evaluation of the normal velocity component. The normal velocity is also particularly susceptible since it involves the x derivative of u and in the solution of region I it was found necessary to supply accurate values of the constants a and b in the initial profile (3.11) to avoid significant errors in the computation of V, even for just one upstream sweep of the region. The constants a and b were calculated from the current $p(x)$ and $g(x)$ profiles using polynomial extrapolation of their values at the five mesh points upstream of x_R. Even so, with $\Delta x = 0{\cdot}1$ the errors in $V(x)$ were found to accumulate to unacceptable proportions after a large number of complete iterations of the flow field, eventually leading to an oscillation in $P(x)$ [despite having comparatively little effect upon $G(x)$] before the system had adequately converged to a final state. Although reduction of Δx improved this, the computational time was correspondingly increased and so a polynomial fitting routine was used to smoothe the profiles of P and G after each iteration. This consisted of least squares approximations to both P and G using polynomials of degree equal to approximately two-thirds of the number of mesh points between x_0 and x_R, ensuring only very slight deviations from the actual function values at the mesh points. This method, which was only a part-time device to aid convergence, was found to be effective and the values of p_1 and x_R converged successfully to limiting values as shown in figure 2. Several relaxation factors were tested, a value of $R = 0{\cdot}8$ providing realistic results within about 30 complete iterations. On average, about 2 or 3 sweeps of region III were required for each complete iteration of the flow field in order to obtain the solution in which $p \to 0$ as $x \to \infty$. In practice this consisted of requiring that p remained

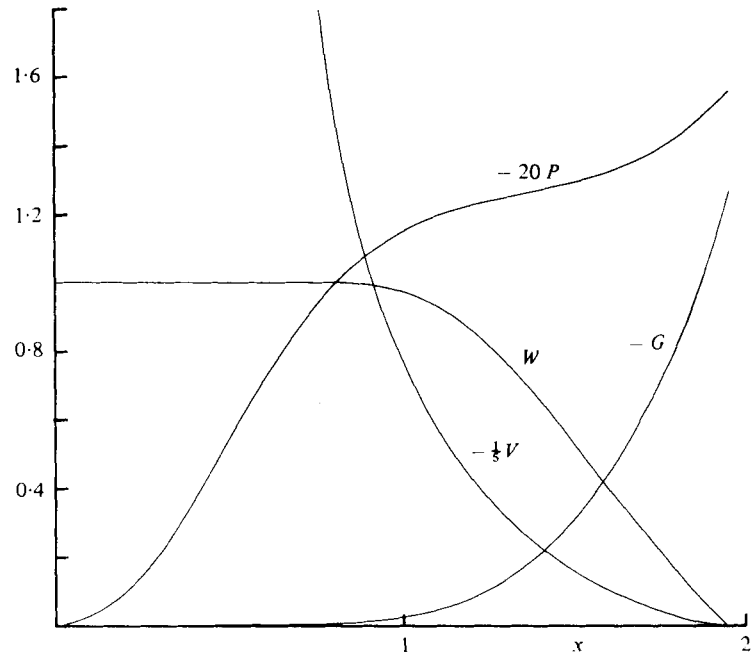

FIGURE 3. The final profiles P, G, V and W.

negative and monotonically increasing to as large a value of x as required (taken as $x = 8$). If p became positive it appeared that a compressive solution evolved as $x \to \infty$ (although an exhaustive search for a solution with a pressure overshoot was not carried out), while $dp/dx < 0$ indicated that an expansive solution would develop downstream.

The final results which are displayed in figures 3–6 were obtained by removing the polynomial fitting routine and also decreasing the step-size in regions I and II to $\Delta x = 0{\cdot}02$. The results obtained from the $\Delta x = 0{\cdot}1$ computations provided accurate initial profiles for $P(x)$ and $G(x)$ and only a few further iterations were required to reduce the difference of successive iterates to less than 5×10^{-4}. The final profiles of P, G, W and V in $0 \leqslant x < x_R$ are shown in figure 3. In figure 6 the velocity profiles show the reattachment of the flow at x_R and it may be seen that the outer boundaries of $\bar{y}$ and y at 7·5 are more than adequate. The final values of x_R and p_1, which are believed to be accurate to two decimal places, were found to be

$$x_R = 1{\cdot}94, \quad p_1 = 0{\cdot}11. \tag{4.2}$$

5. Discussion

It has been confirmed numerically that the system of equations and boundary conditions derived in I has a solution which incorporates reattachment at a distance $O(\epsilon^3 l)$ downstream of the point of intersection of the incoming shear layer and the wall. The precise distance has been found to be

$$x^* = 1{\cdot}94\epsilon^3 M_\infty^{\frac{3}{2}} \lambda^{\frac{1}{4}} (M_\infty^2 - 1)^{-\frac{1}{8}} (\nu_w/\epsilon^8)^{-\frac{1}{4}} \lambda_1^{-\frac{3}{4}}. \tag{5.1}$$

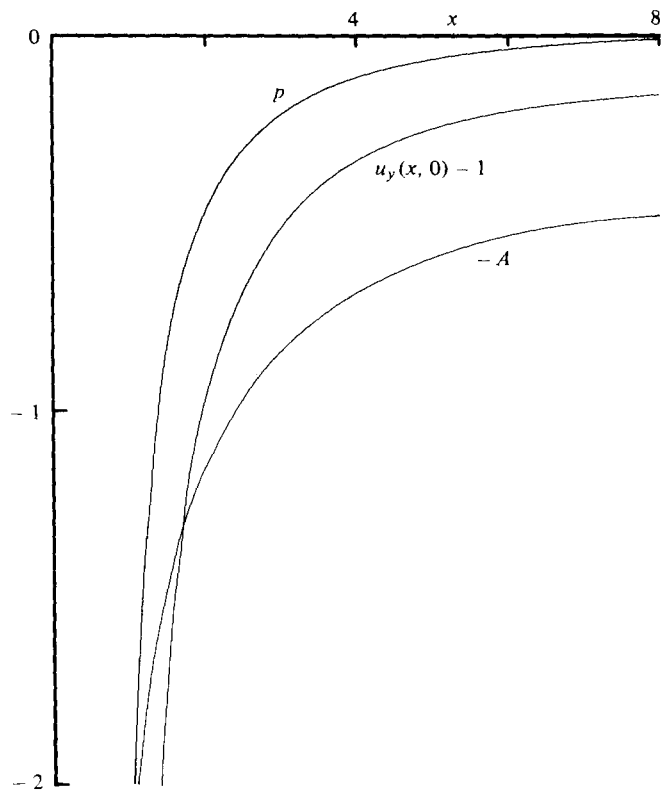

FIGURE 4. Pressure p, skin friction $\partial u/\partial y(x, 0)$ and displacement function A.

The numerical results also predict a positive $O(\epsilon^2)$ correction to the pressure in the inviscid zone just upstream of reattachment, its value where $\epsilon^4 \ll x^*/l \ll \epsilon^3$ being

$$0{\cdot}11\epsilon^2\gamma p_\infty M_\infty (M_\infty^2 - 1)^{-\frac{1}{4}} \lambda_1 \lambda^{-\frac{1}{4}} (\nu_w/\epsilon^8)^{\frac{1}{4}}. \tag{5.2}$$

The results appear to be consistent with the available experimental evidence although a comprehensive comparison is not really possible without a more detailed resolution of the reattachment region in the experiments, and in any case, as pointed out in § 1, the applicability of the theory to any specific flow configuration is by no means proven. Chapman, Kuehn & Larson (1958) present data for separated laminar flows at high Reynolds numbers for a variety of geometries which also incorporate reattachment. These include flows caused by shock-wave boundary-layer interactions, on compression ramps and over backward-facing steps. Additional data for the step configuration is also provided by the experiments of Hama (1968) and Rom (1966), while for the compression ramp, numerical solutions of the full Navier–Stokes equations have been carried out by Carter (1972) and for asymptotically small ramp angles by Burggraf, Jensen & Rizzetta (1975) using triple-deck theory. In all these studies it is generally found that the pressure curve always approaches its limiting value p_∞ through a monotonically increasing variation of the type produced in figure 4; although some experiments show a pressure overshoot, the overall evidence would

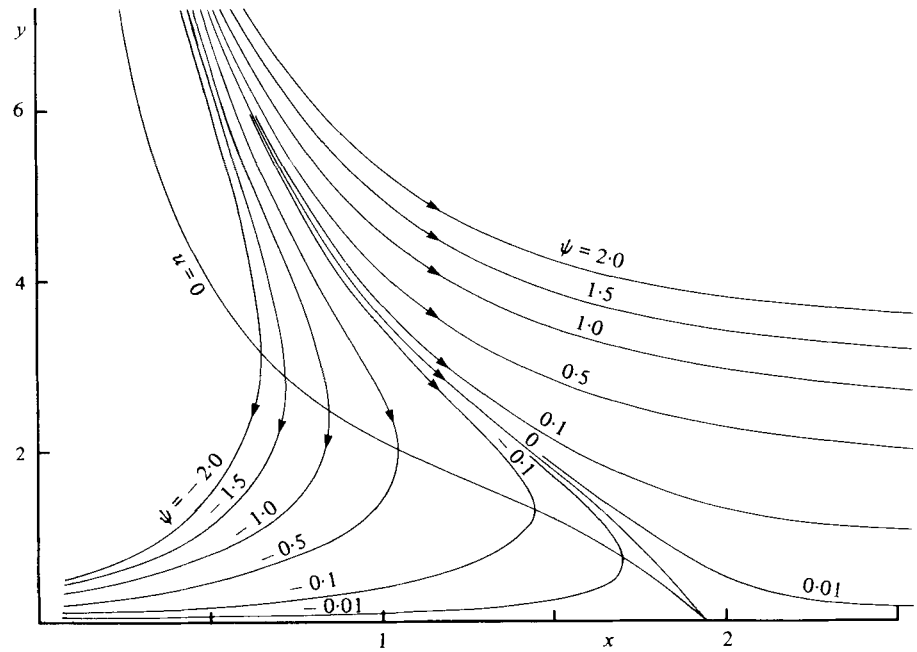

FIGURE 5. Streamlines and the boundary of the reverse flow region, $y = g(x)$.

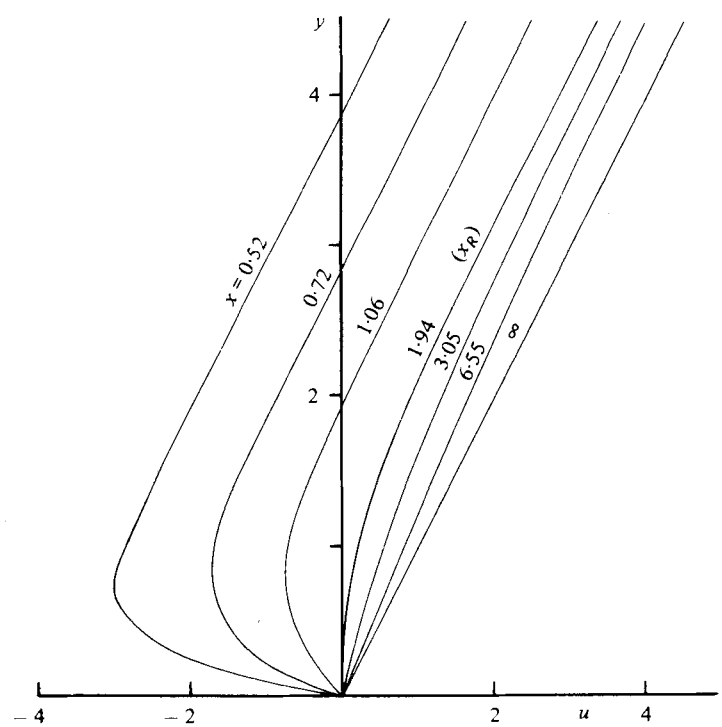

FIGURE 6. Velocity profiles at various values of x.

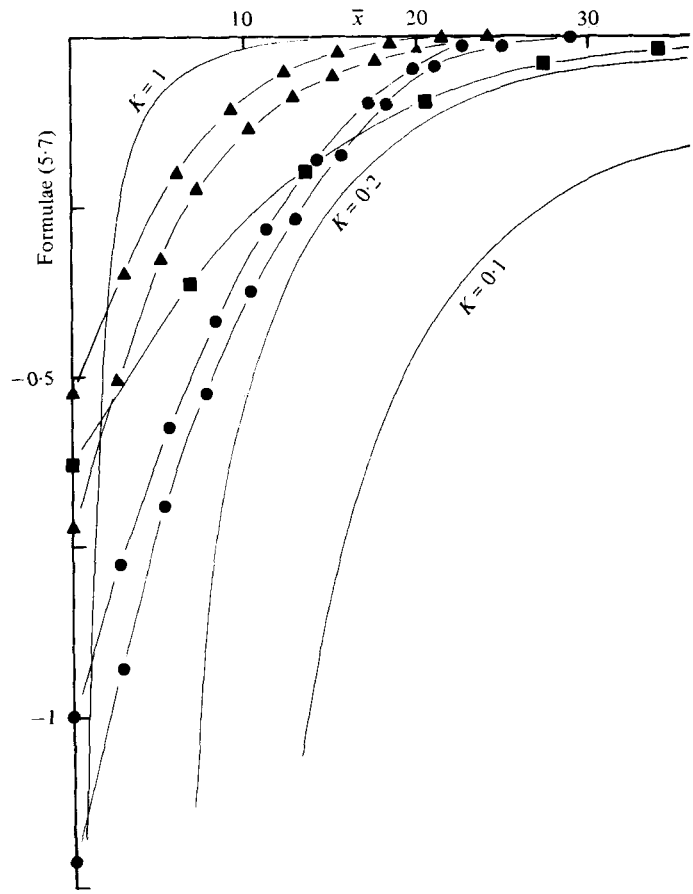

FIGURE 7. Comparison with experiment. Continuous curves give theoretical pressure according to (5.7) and present results for $K = 0{\cdot}1$, $0{\cdot}2$ and $1{\cdot}0$. Experimental data from Chapman *et al.* (1958) and Hama (1968) given by circles (step configuration), triangles (compression ramp) and squares (shock-wave interaction).

indicate that this is possibly experimental error. The large pressure variation predicted by the inviscid zone solution upstream is consistently reproduced in the experiments but it must be remembered that here we are concerned with a much smaller variation which is therefore subject to experimental error to a greater extent.

Despite the reservations made in § 1, a selection of the more consistent experimental results for a range of reattachment problems is compared with the present theoretical results in figure 7. In order to achieve this comparison the values of the constants λ, λ_1 and ν_w must be supplied in (2.1) and (2.8). If we assume a linear viscosity law in which the coefficient of viscosity $\mu = \mu_\infty T/T_\infty$, where T is the temperature of the fluid and T_∞ the temperature external to the triple deck, then

$$\nu_w/\epsilon^8 = U_\infty l T_w^2/T_\infty^2, \tag{5.3}$$

where T_w is the temperature of the wall. If in addition the Prandtl number of the fluid is unity and the wall is thermally insulated, we have

$$\frac{T_w}{T_\infty} = 1 + \frac{\gamma - 1}{2} M_\infty^2, \tag{5.4}$$

where M_∞ is the Mach number of the flow outside the triple deck. In general circumstances the velocity profile U_0 which enters the main deck of the triple deck and which supplies the value of λ will depend upon the temperature, Mach number and geometry of the entire flow upstream of reattachment and thus no simple scaling law for λ or λ_1 is possible. However if the step height or ramp angle are small so that the external Mach number (M_∞) and temperature (T_∞) are approximately constant throughout the flow, then the upstream form of the compressible boundary-layer solution would suggest that we may write

$$\lambda = U_0'(0) = \frac{KU_\infty}{l}\left(\frac{T_\infty}{T_w}\right) = \frac{KU_\infty}{l}\left(1 + \frac{\gamma - 1}{2} M_\infty^2\right)^{-1}, \tag{5.5}$$

where K is a numerical constant (i.e. independent of changes in M_∞, U_∞, T_w etc.). The results of the approximate solution of Messiter *et al.* (1973) for the backward-facing step suggest that for that particular geometry K has a value of about 0·23. For general step heights or ramp angles, we can no longer assume that K will be independent of external conditions, although it always follows from (5.5) that

$$\lambda_1 = M_0'(0) = \frac{KM_\infty}{l}\left(1 + \frac{\gamma - 1}{2} M_\infty^2\right)^{-\frac{3}{2}}, \tag{5.6}$$

and so we may write

$$\left(\frac{p^*}{p_\infty} - 1\right)\frac{(M_\infty^2 - 1)^{\frac{1}{4}}}{\gamma M_\infty^2 \epsilon^2} = K^{\frac{1}{4}} p(K^{\frac{1}{4}}\bar{x}), \tag{5.7}$$

where

$$\left(\frac{x^*}{l}\right)\frac{(M_\infty^2 - 1)^{\frac{3}{8}}}{\left(1 + \frac{\gamma - 1}{2} M_\infty^2\right)^{\frac{3}{2}} \epsilon^3} = \bar{x}. \tag{5.8}$$

We may therefore compare the left-hand side of (5.7), obtained from experiments, with the right-hand side, obtained from the present theory, for various values of K. As can be seen from figure 7 the experimental results for all three types of reattachment problem considered appear to lie within the range $0{\cdot}2 < K < 1$ with a value of K for the step problem fairly consistent with that predicted by the theory of Messiter *et al.* It should be stressed that any quantitative comparison between experimental results and the present theory is difficult to obtain. For instance, in theory the origin of the triple-deck region should be sited at the centre of the inviscid zone whereas in practice this cannot be located from the experimental results with any degree of accuracy; in figure 7 the origin has been chosen somewhat arbitrarily as the point at which one third of the reattachment pressure rise has occurred and of course the triple-deck theory is no longer relevant in this region.

The author is grateful for useful discussions with, and encouragement from, Mr P. G. Williams, Dr P. M. Eagles and Dr P. Bhattacharyya.

REFERENCES

BURGGRAF, O. R. 1970 *U.S. Air Force Aerospace Res. Lab. Rep.* ARL 70-0275.

BURGGRAF, O. R., JENSEN, R. & RIZZETTA, D. P. 1975 *Proc. 4th Int. Conf. Num. Meth. in Fluid Mech., Boulder* 1974, Lecture notes in Physics, vol. 35, p. 218. Springer.

CARTER, J. E. 1972 *N.A.S.A. Tech. Rep.* R-385.

CHAPMAN, D. R., KUEHN, D. M. & LARSON, H. K. 1958 *N.A.C.A. Rep.* no. 1356.

DANIELS, P. G. 1974 *Q. J. Mech. Appl. Math.* **27**, 175.

DANIELS, P. G. 1979 *J. Fluid Mech.* **90**, 289.

FLÜGGE-LOTZ, I. & REYHNER, T. A. 1968 *Int. J. Non-linear Mech.* **3**, 173.

HAMA, F. R. 1968 *A.I.A.A. J.* **6**, 212.

JOBE, C. E. & BURGGRAF, O. R. 1974 *Proc. Roy. Soc.* A **340**, 91.

KLEMP, J. B. & ACRIVOS, A. 1972 *J. Fluid Mech.* **53**, 177.

MESSITER, A. F., HOUGH, G. R. & FEO, A. 1973 *J. Fluid Mech.* **60**, 605.

ROM, J. 1966 *J. Spacecraft & Rockets* **3**, 1504.

SMITH, F. T. 1974 *J.I.M.A.* **13**, 127.

SMITH, F. T. 1977 *Proc. Roy. Soc.* A **356**, 443.

SMITH, F. T. 1979 *J. Fluid Mech.* **90**, 725.

STEWARTSON, K. 1974 *Adv. Appl. Mech.* **14**, 145.

STEWARTSON, K. & WILLIAMS, P. G. 1969 *Proc. Roy. Soc.* A **312**, 181.

WILLIAMS, P. G. 1975 *Proc. 4th Int. Conf. Num. Meth. in Fluid Mech. Boulder* 1974, Lecture notes in Physics, vol. 35, p. 445. Springer.